

# Kleinhospitines A–D, New Cycloartane Triterpenoid Alkaloids from *Kleinhovia hospita*

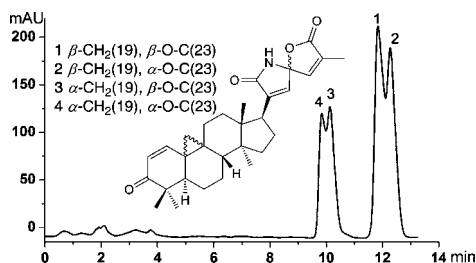
Chang-Xin Zhou,<sup>†</sup> Li Zou,<sup>†</sup> Li-She Gan,<sup>\*,†</sup> and Yue-Lan Cao<sup>‡</sup>

College of Pharmaceutical Sciences, Zhejiang University, 866 Yuhangtang Road, Hangzhou 310058, P. R. China, and Department of Dermatology, Second Affiliated Hospital of Zhejiang University, 88 Jiefang Road, Hangzhou 310009, P. R. China

lsgan@zju.edu.cn

Received April 17, 2013

## ABSTRACT



Kleinhospitines A–D, four unprecedented cycloartane triterpenoid alkaloids possessing a spiro  $\alpha,\beta$ -unsaturated  $\gamma$ -lactam lactone side chain, were isolated as two mixtures of C-23 epimers from *Kleinhovia hospita*. Kleinhospitines C and D represent the first examples of naturally occurring cycloartane triterpenoids with a  $9\alpha,10\alpha$ -cyclopropyl ring. The structures and absolute configurations were determined on the basis of spectroscopic analyses and comprehensive quantum chemical calculations. The two mixtures showed hepatoprotective activity against  $H_2O_2$ -induced oxidative damages on primary cultured rat hepatocytes with  $EC_{50}$  values of 167.0 and 126.5  $\mu$ M.

The first cycloartane triterpenoid, cycloartenone, was isolated from the fruits of *Artocarpus integrifolia* in the 1930s and later structurally identified mainly by chemical methods and an IR spectrum in the 1950s.<sup>1</sup> Cycloartenol, the corresponding alcohol of cycloartenone, was later found to be a key intermediate in the biosynthesis of phyto-steroids.<sup>2</sup> Cycloartenol and its weakly polar derivatives are widely distributed in plants, yet its highly oxidized products are so rare that an unsubstituted C-21 methyl was once believed to be characteristic of cycloartane triterpenoids.<sup>3</sup> However, as more cycloartane triterpenoids were discovered, oxidation at almost every carbon of the side chain and the main tetracyclic rings were found.

Some complicated 9,10-*seco* nortriterpenoid derivatives were also isolated from the genus *Schisandra*,<sup>4</sup> and cycloartane-type triterpenoid alkaloid derivatives were reported to occur in the genus *Buxus* and *Cimicifuga*.<sup>5</sup>

As continuous work on the hepatoprotective cycloartane triterpenoids from *Kleinhovia hospita* (Sterculiaceae),<sup>6</sup> the plant material was reinvestigated. A mixture with highly oxidized structures, as indicated by <sup>1</sup>H NMR, was first isolated by silica gel column chromatography from an EtOAc soluble fraction of the 95% EtOH extract of *K. hospita*. LC-MS/TOF analysis of the mixture showed two closely adjacent peaks with similar MS spectra (see Supporting Information (SI), Figure S31). With optimized HPLC solvent conditions (65% MeCN, RP C-8 column,

<sup>†</sup> College of Pharmaceutical Sciences, Zhejiang University.

<sup>‡</sup> Second Affiliated Hospital of Zhejiang University.

(1) (a) Barton, D. H. R. *J. Chem. Soc.* **1951**, 1444–1451. (b) Bentley, H. R.; Henry, J. A.; Irvine, D. S.; Spring, F. S. *J. Chem. Soc.* **1953**, 3673–3678. (c) Barton, D. H. R.; Page, J. E.; Warnhoff, E. W. *J. Chem. Soc.* **1954**, 2715–2719.

(2) Benveniste, P.; Hewlins, M. J. E.; Fritig, B. *Eur. J. Biochem.* **1969**, 9, 526–533.

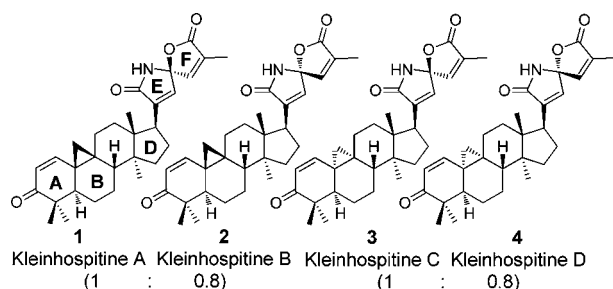
(3) Boar, R. B.; Romer, C. R. *Phytochemistry* **1975**, 14, 1143–1146.

(4) Xiao, W. L.; Li, R. T.; Li, S. H.; Li, X. L.; Sun, H. D.; Zheng, Y. T.; Wang, R. R.; Lu, Y.; Wang, C.; Zheng, Q. T. *Org. Lett.* **2005**, 7, 1263–1266.

(5) (a) Nakano, T.; Terao, S. *J. Chem. Soc.* **1965**, 4512–4537. (b) Dan, C.; Zhou, Y.; Ye, D.; Peng, S.; Ding, L.; Gross, M. L.; Qiu, S. X. *Org. Lett.* **2007**, 9, 1813–1816.

(6) Gan, L. S.; Ren, G.; Mo, J. X.; Zhang, X. Y.; Yao, W.; Zhou, C. X. *J. Nat. Prod.* **2009**, 72, 1102–1105.

250 mm  $\times$  4.6 mm, 5  $\mu$ m), the mixture was resolved into two double peaks and separated into two groups of epimers. The structures of each epimeric pair were finally elucidated by a combination of spectroscopic and quantum chemical methods including 2D NMR and DFT quantum chemical calculations of the theoretical ECD, OR, and  $^1\text{H}$  and  $^{13}\text{C}$  NMR data. We report herein the isolation, structure determination, and hepatoprotective activities of these compounds.



Kleinhospitines A (**1**) and B (**2**)<sup>7</sup> were isolated together as a white amorphous powder (4 mg from 8 kg of plant material) and showed the same molecular formula of  $\text{C}_{30}\text{H}_{38}\text{NO}_4$ , as indicated by a positive LC-HRESIMS pseudomolecular ion peak at  $m/z$  476.2788 [ $\text{M} + \text{H}$ ]<sup>+</sup> (calcd 476.2801) (Figure S31). Comparison of the IR spectrum with those of the known spiro-cycloartane triterpenoids in our previous study showed that, besides two characteristic absorption peaks for the  $\alpha,\beta$ -unsaturated ketone of ring A (1667  $\text{cm}^{-1}$ ) and the  $\alpha,\beta$ -unsaturated  $\gamma$ -lactone group of ring F (1778  $\text{cm}^{-1}$ ),<sup>6</sup> an additional absorption peak at 1725  $\text{cm}^{-1}$  indicated the presence of another unsaturated lactone or lactam for **1** and **2**. Two intercoupling olefinic hydrogens at  $\delta_{\text{H}}$  7.01 (H-1) and 5.94 (H-2) (both d,  $J = 10.2$  Hz), a quartet at  $\delta_{\text{H}}$  6.96 (for **1**) or 6.98 (for **2**) (both q,  $J = 1.6$  Hz, H-24), and a singlet at 1.95 (br s,  $\text{H}_3$ -26) in the  $^1\text{H}$  NMR spectrum were also supportive for the presence of similar rings A and F in the two compounds. An additional singlet at  $\delta_{\text{H}}$  6.61 (for **1**) or 6.60 (for **2**) suggested the existence of another trisubstituted double bond (Table S2). The  $^{13}\text{C}$  NMR showed, apart from several clearly isolated signals, split but very close signals for most carbons, which also indicated that the powder was a mixture of two closely related structures. Comparison of their  $^{13}\text{C}$  NMR data with those of the known spiro-cycloartane triterpenoids<sup>6</sup> showed that the original acetal carbon signal for C-21 vanished and an extra unsaturated lactone or lactam carbon signal at  $\delta_{\text{C}}$  174.3 (174.4) as well as two olefinic carbon signals were observed. The spiro carbon signal was upfield-shifted from ca.  $\delta_{\text{C}}$  110 to 95.5 (96.0) (Table S1). The above data suggested a spiro-cycloartane triterpenoid with an  $\alpha,\beta$ -unsaturated  $\gamma$ -lactam E ring for **1** and **2**. The structural

(7) **Kleinhospitines A and B** in a mixture (**1:2** = 1:0.8): White amorphous powder;  $[\alpha]_{\text{D}}^{20} +22$  (c 0.40, MeOH); UV (MeOH)  $\lambda_{\text{max}}$  (log  $\epsilon$ ) 267 (3.81), 211 (4.17) nm; CD (MeOH)  $\lambda_{\text{max}}$  ( $\Delta\epsilon$ ) 339 (−0.68), 303 (+0.20), 252 (−1.33), 220 (+3.63) nm; IR (KBr)  $\nu_{\text{max}}$  3328, 2925, 2854, 1778, 1725, 1667, 1604, 1463, 1380, 1151, 991  $\text{cm}^{-1}$ ;  $^1\text{H}$  and  $^{13}\text{C}$  NMR, see Tables S1 and S2 (S1); ESIMS (positive)  $m/z$  476 [ $\text{M} + \text{H}$ ]<sup>+</sup>, 951 [ $2\text{M} + \text{H}$ ]<sup>+</sup>; ESIMS (negative)  $m/z$  474 [ $\text{M} - \text{H}$ ]<sup>−</sup>; HRESIMS  $m/z$  476.2788 (calcd for  $\text{C}_{30}\text{H}_{38}\text{NO}_4$ , 476.2801).

differences of the two isomers may lie in the configuration at the spiro carbon C-23.

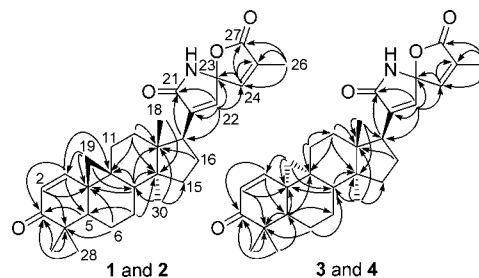


**Figure 1.** Key HMBC ( $\text{H} \rightarrow \text{C}$ ) correlations of kleinhospitines A–D.

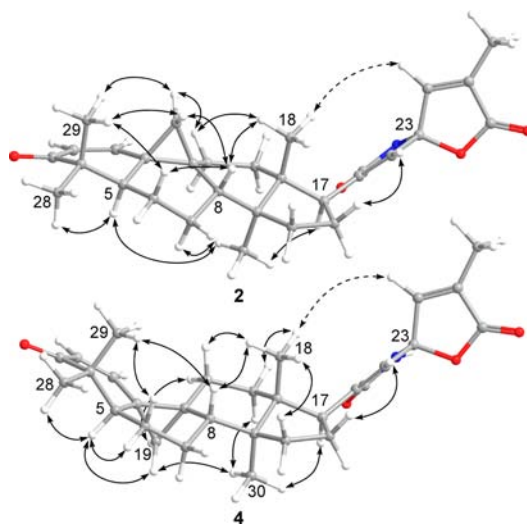


**Figure 2.** Key NOESY correlations represented by **2** and **4** (solid arrows were also observed for **1** and **3**).

Careful analyses of the HSQC, HMBC, and NOESY spectra unambiguously allowed assignments of the  $^1\text{H}$  and  $^{13}\text{C}$  signals (Tables S1 and S2) of **1** and **2**. In the HMBC spectrum, key correlations from H-22 to C-20, C-21, C-17, C-23, and C-24 (Figure S13), as well as the correlation from H-17 to C-21, confirmed the  $\alpha,\beta$ -unsaturated  $\gamma$ -lactam ring E (Figure 1). In the NOESY spectrum, correlations of  $\text{H}_3$ -18/H-8, H-8/H<sub>2</sub>-19, and H<sub>2</sub>-19/ $\text{H}_3$ -29 indicated their  $\beta$ -orientation, while correlations of  $\text{H}_3$ -28/H-5 and H-5/ $\text{H}_3$ -30 suggested that these hydrogens were all  $\alpha$ -facial. Meanwhile, the NOESY correlation of  $\text{H}_3$ -18/H-24 observed only for compound **2** suggested an *R*- and

(8) **Kleinhospitines C and D** in a mixture (**3:4** = 1:0.8): White amorphous powder;  $[\alpha]_{\text{D}}^{20} -68$  (c 0.25, MeOH); UV (MeOH)  $\lambda_{\text{max}}$  (log  $\epsilon$ ) 270 (3.71), 209 (4.02) nm; CD (MeOH)  $\lambda_{\text{max}}$  ( $\Delta\epsilon$ ) 322 (+1.51), 269 (−6.75), 221 (+2.63) nm; IR (KBr)  $\nu_{\text{max}}$  3332, 2926, 2855, 1777, 1726, 1668, 1612, 1463, 1384, 1193, 992  $\text{cm}^{-1}$ ;  $^1\text{H}$  and  $^{13}\text{C}$  NMR, see Table S1 and S2 (S1); ESIMS (positive)  $m/z$  476 [ $\text{M} + \text{H}$ ]<sup>+</sup>, 973 [ $2\text{M} + \text{Na}$ ]<sup>+</sup>; HRESIMS  $m/z$  476.2793 (calcd for  $\text{C}_{30}\text{H}_{38}\text{NO}_4$ , 476.2801).

S-configuration for the spiro carbon C-23 of **1** and **2**, respectively (Figures 2 and S16). As indicated by the integration values of the most distinguishable signals of H-24, H-22, and H<sub>3</sub>-18 in the <sup>1</sup>H NMR spectrum, **1** and **2** are obtained in a ratio of about 1:0.8.

Kleinhospitines **3** (**3**) and **4** (**4**),<sup>8</sup> represented by the first twin peak in HPLC, were isolated together as a white amorphous powder (2 mg from 8 kg of plant material) and showed the same molecular formula as those of **1** and **2**. The IR spectrum also showed high similarity with that of the mixture of **1** and **2**. Comparison of the <sup>1</sup>H NMR data of the two mixtures showed that H-1 of **3** and **4** was upfield shifted to  $\delta_{\text{H}}$  6.63 (and 6.62) (d,  $J$  = 10.2 Hz) and the H-19b was downfield shifted to  $\delta_{\text{H}}$  0.97 (d, 2H,  $J$  = 4.8 Hz). Little difference can be observed from the <sup>13</sup>C NMR spectrum (Table S1), except for the most distinguishable carbon signals for C-1 and C-2 at  $\delta_{\text{C}}$  159.9 and 124.6. The above data suggested that **3**(**4**) and **1**(**2**) are different in the configurations on ring A or the cyclopropane ring. This deduction puts forward a new challenge regarding the fact that configurations for the A, B, C, D, and the cyclopropane rings of the cycloartane triterpenoid remain intact since the discovery of these natural products. Further analysis of their 2D NMR (HSQC, HMBC, and NOESY) (Figures 1 and 2) data revealed that the two pairs of isomers shared the same planar structure and the same stereochemistry of rings D, E, and F. However, NOESY correlations H<sub>3</sub>-28/H-5, H-5/H-19a, H-19a/H<sub>3</sub>-30, H<sub>3</sub>-30/H-17, H<sub>3</sub>-18/H-8, and H-8/H<sub>3</sub>-29 showed that H<sub>3</sub>-28, H-5, H-19a, H<sub>3</sub>-30, and H-17 were  $\alpha$ -oriented, while H<sub>3</sub>-18, H-8, and H<sub>3</sub>-29 were  $\beta$ -facial hydrogens. These observations suggested that compounds **3** and **4** had a unique  $\alpha$ -cyclopropane ring, and they differed from **1** and **2** only in the configuration of the cyclopropane ring. **3** and **4** are the first two naturally occurring cycloartane triterpenoids that had an  $\alpha$ -cyclopropane ring.

In order to further confirm the difference between **1**(**2**) and **3**(**4**), ECD spectra of the two mixtures were measured, and the results showed a first negative Cotton effect at 339 nm for **1**(**2**) and, conversely, a first positive one at 322 nm for **3**(**4**) (Figures 3 and 5). Based on the above findings, the structures of **1** and **2** were studied theoretically by TDDFT calculations of their ECD spectra following our previously reported procedures.<sup>9</sup> Conformational analyses of **1** and **2** in the SPARTAN 04 software package<sup>10</sup> resulted in two lowest energy conformers for each (**1C1**, **1C2**, **2C1**, **2C2**, Figure S32) due to the free rotation of the C-17–C-20 bond. Subsequently, ECD spectra for each of the conformers were calculated at the B3LYP/6-311++G(2d,2p)//B3LYP/6-31+G(d) level by the GAUSSIAN 09 program.<sup>11</sup> The ECD spectra were then simulated by the overlapping Gaussian function.<sup>12</sup> The calculated ECD spectra of both **1** and **2** showed a

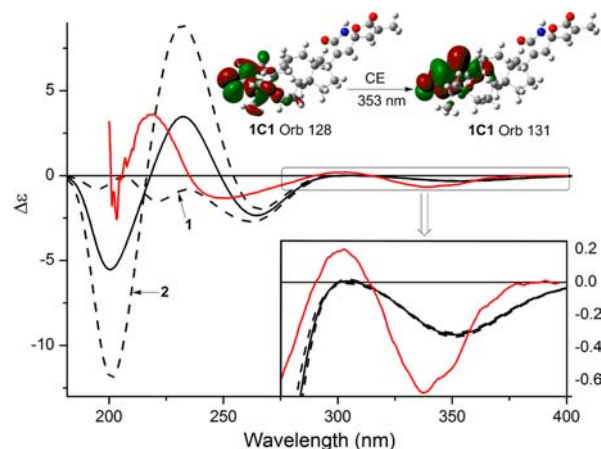


**Figure 3.** Experimental ECD spectrum of **1** and **2** in mixture (solid red line), B3LYP/6-311++G(2d,2p)//B3LYP/6-31+G(d) calculated ECD curves of **1** and **2** (dash line) and the 1:0.8 weighted one (solid black line), and the key molecular orbitals involved in the first Cotton effect of **1** and **2** (represented by conformer **1C1**).

negative first Cotton effect around 350 nm (Figure 3). In the 200–250 nm range, the negative Cotton effect around 220 nm for **1** and the positive Cotton effect around 230 for **2** may be attributed to their different configurations at C-23, and the experimental positive Cotton effect at 220 nm for the mixture can be appropriately simulated by weighting their percentages. Furthermore, the key molecular orbital involved in the first negative Cotton effects around 350 nm of **1C1** were also calculated, and their localization around ring A and the cyclopropane ring were observed. Since **3** and **4** both had a first positive Cotton effect, this observation was also in agreement with the conclusion that **3**(**4**) differed from **1**(**2**) in the configuration of the cyclopropane ring.

TDDFT calculations of the theoretical ECD spectra of **3** and **4**, as well as the theoretical <sup>1</sup>H and <sup>13</sup>C NMR chemical shifts and the optical rotation (OR) of **1**–**4**, were further carried out. Unfortunately, conformational analysis of **3** by Spartan 04 software gave two lowest energy conformers (**3C1**, **3C2**), but none of them could satisfy the experimental NOESY correlations of H<sub>3</sub>-29/H-8, H<sub>3</sub>-29/H-6a, and H-6b/H-5. Besides, ECD and NMR calculations also failed to provide matchable data (Figure S34, Table S5). Therefore, the lowest energy conformers of **3** and **4** were then adjusted manually based on NOESY findings. The adjusted conformers (**3Cm**, **4Cm**) were reoptimized by Gaussian 09 at the same level and showed much lower relative Gibbs free energy than those given by Spartan 04 software (Figure 4).

Compared to the experimental ECD spectrum of the **3** and **4** in mixture, the calculated spectra both showed a corresponding positive first Cotton effect around 325 nm. In the 200–250 nm range, similar to those of **1** and **2**, a negative Cotton effect around 220 nm for the 23*R* configuration (**3**) and a positive one around 230 for the 23*S*

(9) Gan, L. S.; Zheng, Y. L.; Mo, J. X.; Liu, X.; Li, X. H.; Zhou, C. X. *J. Nat. Prod.* **2009**, *72*, 1497–1501.

(10) *Spartan 04*; Wavefunction Inc.: Irvine, CA.

(11) *Gaussian 09*, revision A.1; Gaussian, Inc.: Wallingford, CT, 2009. Full list of authors can be found in the SI.

(12) Stephens, P. J.; Harada, N. *Chirality* **2010**, *22*, 229–233.



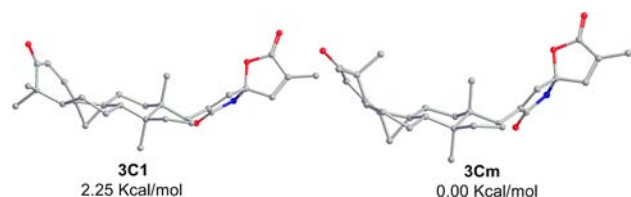


**Figure 4.** B3LYP/6-31+G(d) optimized lowest energy 3D conformers (without hydrogens) of **3** and their relative Gibbs free energies (**3C1**, given by Spartan; **3Cm**, created by manual adjustment of **3C1**).

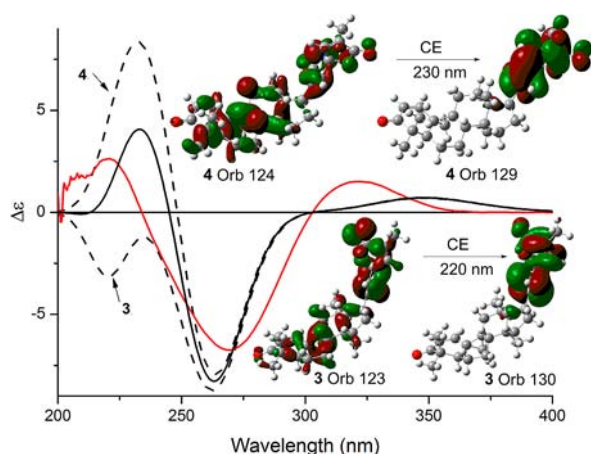


**Figure 5.** Experimental ECD spectrum of **3** and **4** in mixture (solid red line), B3LYP/6-311++G(2d,2p)//B3LYP/6-31+G(d) calculated ECD of **3** and **4** (dash lines) and the 1:0.8 weighted one (solid black line), and the key molecular orbitals involved in the characteristic Cotton effects of **3** and **4**.

configuration (**4**) can be predicted and the experimental Cotton effects can be simulated by weighting both curves with the ratio 1:0.8 (Figure 5).

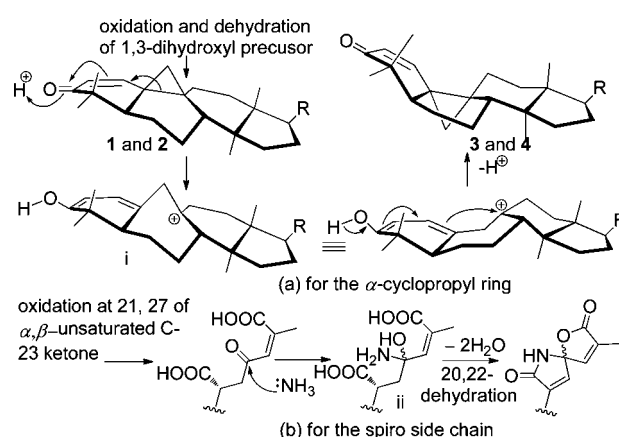
Calculations of specific optical rotations at the B3LYP/6-311++G(2d,2p)//B3LYP/6-31+G(d) level resulted in +22.05, +142.1, −125.95, and −3.09 for **1–4**, respectively. The experimental OR values of +22 for **1(2)** and −68 for **3(4)** can be simulated respectively as +75 and −71 by weighting their theoretical data with their percentages (Table S3).

Compared to the experimental  $^1\text{H}$  NMR chemical shifts for the most different hydrogens of **1(2)** and **3(4)**, H-1 and H-19b, the rmpw1pw91/6-311++G(d,p)//B3LYP/6-31+G(d) calculated ones showed good agreements (Table S4). The calculated  $^{13}\text{C}$  NMR chemical shifts also showed closely related results (Tables S5–S7).

Scheme 1 illustrates the proposed biosynthetic pathway of **1–4**, especially the formation of the  $\alpha$ -cyclopropane ring in **3** and **4** from a 1,3-dihydroxy cycloartane triterpenoid

precursor that was widely found in cycloartane triterpenoids containing plants.<sup>6,13</sup> Acid-aided protonation of the  $\alpha,\beta$ -unsaturated ketone and opening of the cyclopropane ring of compounds **1** and **2** generated a cation intermediate (i), while reformation of the cyclopropane ring by exo attack would yield an  $\alpha$ -cyclopropane ring as in compounds **3** and **4**, respectively. The spiro  $\alpha,\beta$ -unsaturated  $\gamma$ -lactam lactone side chain may originate from oxidation at C-21 and C-27 of the  $\alpha,\beta$ -unsaturated C-23 ketone precursor<sup>6</sup> and further a reductive amination with no stereoselectivity of the ketone by an amide group to form an intermediate (ii), followed by lactonization and 20,22-dehydration. Compared to the known cycloartane-type triterpenoid alkaloids,<sup>5</sup> **1–4** contain a N-atom solely on their complete side chain.

**Scheme 1.** Proposed Biosynthetic Pathway for Compounds **1–4**



Hepatoprotective effects of the two mixtures of **1(2)** and **3(4)** were evaluated on a primary cultured rat hepatocytes damage model induced by  $\text{H}_2\text{O}_2$ , using procedures similar to those previously reported.<sup>9</sup> The two mixtures of **1(2)** and **3(4)** showed hepatoprotective activity with  $\text{EC}_{50}$  values of 167.0 and 126.5  $\mu\text{M}$ , respectively. The positive control, *N*-acetyl-L-cysteine, showed an  $\text{EC}_{50}$  value of 105.6  $\mu\text{M}$ .

**Acknowledgment.** Financial support from the Specialized Program for New Drug Creation and Development of 12th Five-year Plan (No. 2011ZX09102-002-07), the Foundation from Zhejiang Provincial Administration of Traditional Chinese Medicine (No. 2012ZZ009), and Science and Technology Foundation of Zhejiang Province (No. 2009C33135) are gratefully acknowledged.

**Supporting Information Available.** Full experimental procedures; tabulated NMR data; and 1D and 2D NMR, MS, IR spectra of **1(2)** and **3(4)**; the TOF LC-MS spectra of the crude mixture; and the theoretical calculation details were provided. This material is available free of charge via the Internet at <http://pubs.acs.org>.

(13) Gutierrez-Lugo, M. T.; Singh, M. P.; Maiese, W. M.; Timmermann, B. N. *J. Nat. Prod.* **2002**, *65*, 872–875.